

# Optimizing the Thickness Uniformity of Magnetron Sputtering Deposited Films on a Large-Scale Curved Workpiece Surface

Zhao JIANG, Zhenlin WANG \*, Shuilian LUO, Zhanji MA, Yanchun HE, Jian XU

Science and Technology on Vacuum Technology and Physics Laboratory, Lanzhou Institute of Physics, Lanzhou 730000, China

<http://doi.org/10.5755/j02.ms.35103>

Received 14 September 2023; accepted 24 December 2023

This study prepared magnetron-sputtering deposition film on a large-scale curved workpiece with a favorable thickness uniformity using a rectangular target cathode. For a substrate rotation structure with eccentric rotation/revolution composite motion, the geometrical model of the thickness distribution of the coating film on a large substrate was established in combination with the principle of rectangular cathode magnetron sputtering. The integral formula of the film thickness was derived, and various film thickness distribution patterns under different parameters were simulated. According to the present research results, the film thickness distribution can be optimized by adjusting the revolution-to-rotation radius and eccentric ratios. At an eccentric distance of 400 mm and a radius ratio of 2.78, the most favorable uniformity degree of 0.87 was obtained, which was controlled by the motion path of the fixed point on the substrate. The proposed approach helps to obtain large-scale films with favorable uniformity on the substrate.

**Keywords:** film thickness uniformity, magnetron sputtering, large-scale curved workpiece, simulated calculation.

## 1. INTRODUCTION

The uniformity of the film thickness reflects the change in the film coated on the substrate with the position of the substrate in the vacuum chamber. The uniformity directly affects the stability and reliability of various devices [1–4]. In recent years, scholars worldwide have conducted a great deal of research on the thickness distribution of films deposited via magnetron sputtering. For rectangular targets, scholars have mainly emphasized some geometrical parameters, including the target-substrate distance, the rotation of the substrate, and the shape of the target, on the uniformity of film thickness [5–12]; however, there are still great difficulties regarding the uniform preparation of large-area films on large-scale complex components [13, 14]. The present study aims to substantiate the possibility of enhancing the uniformity of film thickness by introducing the eccentric arrangement of the sputtering target, the substrate, and the planetary structure so that the substrate can simultaneously achieve revolution and rotation. A numerical simulation is also performed to provide guidance for actual engineering applications.

## 2. ESTABLISHMENT OF THE THEORETICAL MODEL

### 2.1. Physical model of workpiece gearing

This study adopted a planetary substrate holder, with a revolution motor transferring the rotation to the revolution axis via the worm-gear reduction device, as shown in Fig. 1.

The axis of revolution was located in the center, on which the center gear was fixed. The center of the substrate holder was at the eccentric position, which was supported

by the driven shaft and fixed by the bearing. The rotation gear was fixed with the gear via the driven shaft, and the revolution axis was connected with the fixed mechanism to drive the rotation of the driven shaft and finish the eccentric rotation. The rotation gear and the center gear were engaged to complete the rotation of the substrate. The ratio of the revolution radius to the rotation radius (i.e., the rotation velocity and the revolution velocity) can be set following actual requirements to change the motion path of the point on the substrate. Accordingly, the distribution uniformity of film thickness can be enhanced. As shown in Fig. 2, for a workpiece with a circular curved structure, the radius was 2000 mm, the distance between the coated workpiece and the target  $H$  was 150 mm, the revolution radius was 3500 mm, and the target was 2200 mm × 150 mm in size.

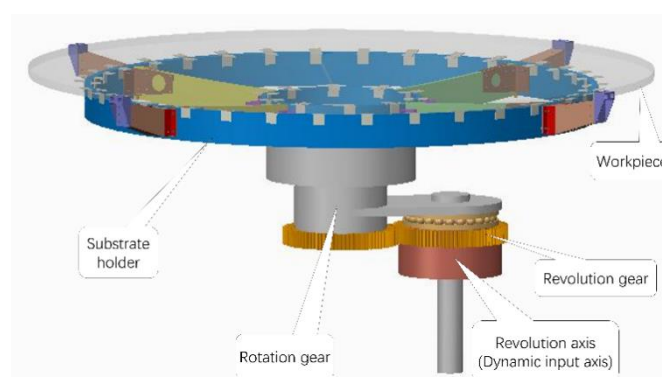


Fig. 1. Illustration of the planetary substrate holder

\*Corresponding author: Tel.: +86-0931-4585027;  
E-mail: [crossir@163.com](mailto:crossir@163.com) (Z. Wang)

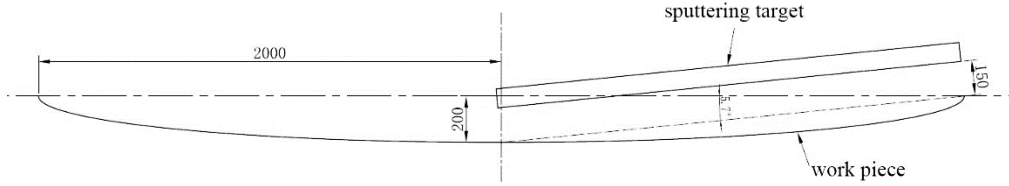


Fig. 2. Illustration of the target-substrate structure

## 2.2. Modeling of the magnetron sputtering process

The following assumptions were used for modeling the rectangular planar magnetron sputtering process to calculate the uniformity of the sputtering-formed film thickness [15–18].

1. The target is subjected to uniform sputtering, i.e., the effect induced by the distortion of the edge electromagnetic field can be ignored. Based on the relation between the erosion phenomenon of the magnetron-sputtering target and the magnetic field, it can be assumed that the sputtering rate of the magnetron-sputtering system is proportional to the horizontal components of the magnetically controlled magnetic field on the target surface.
2. The incident ions are focused on the region near the target surface and accelerated by the electric field, accompanied by enhanced energy. The electric field on the surface of the cathode target is perpendicular to the cathode surface. Accordingly, the ions enter the target surface vertically. It can be assumed that the incident angle of ions equals 0.
3. The sputtered film atoms show no diffusion when sputtered to the substrate. The film atoms stay where they were sputtered and directly participate in film formation. It can thus be assumed that the departure angles of the sputtered film atoms from the target surface obey a simple cosine distribution, i.e., the angle distribution can be described by  $\cos(\beta)$ , in which  $\beta$  is the incident angle.
4. Since the working gas should be filled during the sputtering process, the scattering of the outgoing particles by the gas atoms during the flight from the target to the substrate cannot be ignored. However, the pressure of the working gas is typically less than one pascal, which can be regarded as a rarefaction state. It can be assumed that the outgoing particles are scattered during the space flight process, and the deposition probability on the substrate is inversely proportional to the path length.

The above four assumptions cannot impose great errors on the derivation. The geometrical model was established, as shown in Fig. 3. Based on the above assumptions, by assuming that  $P$  is the sputtering rate of the magnetron sputtering system, the number of particles sputtered from any element on the target surface  $dA$  to the element on the substrate  $dB$  can be derived as follows:

$$dN = P \cos(\beta) dA d\omega / \pi, \quad (1)$$

where  $\beta$  is the inclination angle between the normal direction of the target element  $dA$  and the line connecting  $dA$  and  $dB$ ,  $d\omega$  is the solid angle ( $d\omega = dB \cos(\varphi) / L^2$ ),  $\varphi$  is the intersection angle between the normal direction of  $dB$  and

the line connecting  $dA$  and  $dB$ . For the used directions of the sputtering target and the substrate,  $\varphi = \beta$ .

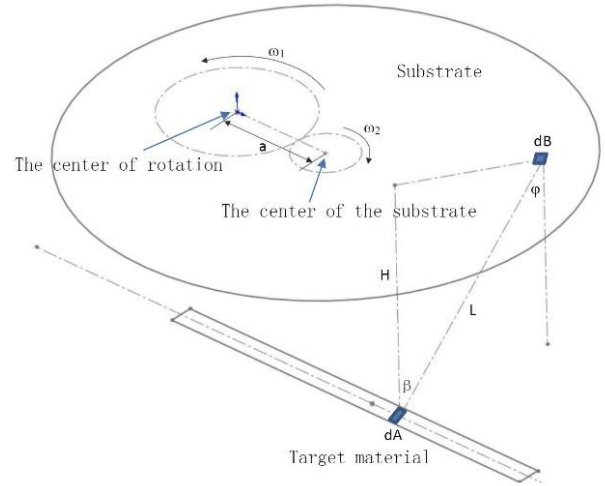


Fig. 3. Illustration of the geometrical model of the sputter coating process

## 3. ANALYSIS OF MODEL CALCULATION

### 3.1. Static thickness distribution

Based on the above 4th assumption, the number of particles sputtered from any element on the target surface  $dA$  to the substrate element  $dB$  can be written as:

$$dN_0 = P \cos^2(\beta) dA dB / (\pi L^2), \quad (2)$$

where  $L$  is the distance between two elements. Assuming that  $\rho$  is the target density and  $T$  is the distribution function of film thickness, the following expression can be derived:

$$dN_0 = \rho dT dB. \quad (3)$$

The distribution function of the film thickness at point  $B$  on the substrate surface can be written as:

$$T = \int P \cos^2(\beta) dA / (\pi \rho L^2). \quad (4)$$

At a distance between the target and the substrate  $H = 150$  mm, the film thickness distribution function pattern was solved with MATLAB, and the results are shown in Fig. 4.

It can be observed from Fig. 4 that the normalized particle deposition density in the selected integral region well described the distribution of film thickness.  $x$ -axis), especially with favorable uniformity in the target length range ( $-1000$  mm  $\sim$   $+1000$  mm). In contrast, the film thickness differed greatly in the region exceeding the target length and showed quite a violent change along the direction of the short side ( $y$ -axis). Overall, the film thickness showed poor uniformity. This observation aligns

with the expectations based on the physical principles of magnetron sputtering, but contrasts with some earlier studies that reported more uniformity along the target width direction.

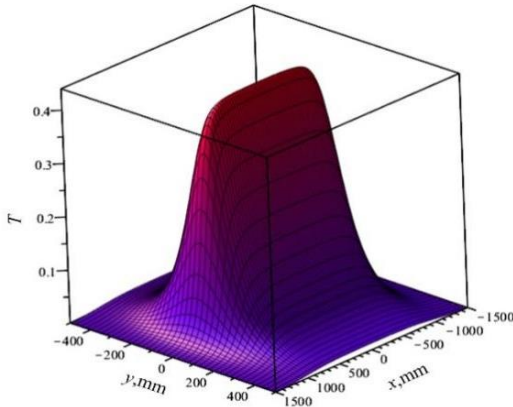


Fig. 4. Distribution pattern of the static relative film thickness on the substrate

### 3.2. Motion path of the substrate

As shown in Fig. 5, based on the geometrical size, the 3D surface equation of the substrate can be obtained as follows:

$$z = (x^2 + y^2) / 2000. \quad (5)$$

Since any point on a substrate is in plane motion,  $z$  is constant. The following vector can describe the position of the point on the substrate:

$$p = \begin{bmatrix} x \\ y \\ 1 \end{bmatrix}. \quad (6)$$

The position transform matrix of any point during the rotation of the substrate can be written as follows:

$$R_2 = \begin{bmatrix} \cos(\omega_2 t) & -\sin(\omega_2 t) & 0 \\ \sin(\omega_2 t) & \cos(\omega_2 t) & 0 \\ 0 & 0 & 1 \end{bmatrix}. \quad (7)$$

The distance between the rotation axis of the substrate and the revolution axis can be described by the translation matrix:

$$D = \begin{bmatrix} 1 & 0 & a \\ 0 & 1 & 0 \\ 0 & 0 & 1 \end{bmatrix}. \quad (8)$$

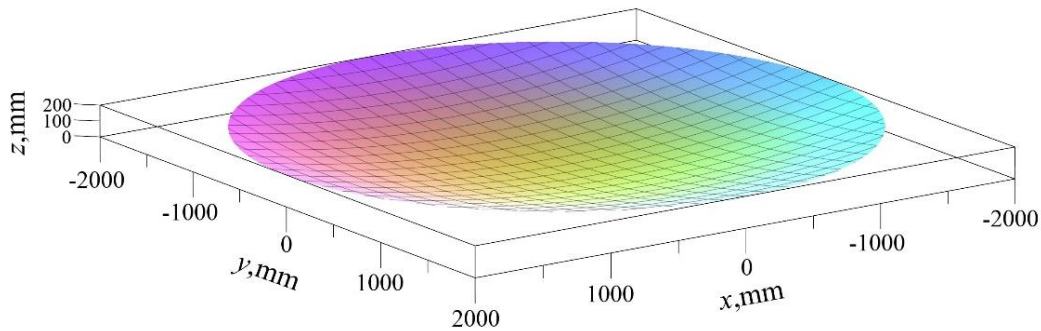


Fig. 5. 3D model of the substrate

The position transform matrix of any point during the revolution of the substrate can be written as:

$$R_1 = \begin{bmatrix} \cos(\omega_1 t) & -\sin(\omega_1 t) & 0 \\ \sin(\omega_1 t) & \cos(\omega_1 t) & 0 \\ 0 & 0 & 1 \end{bmatrix}. \quad (9)$$

Assuming that  $\omega_1$  and  $\omega_2$  are the angular velocities of revolution and rotation, respectively,  $t$  is the time function, and  $\kappa$  is the revolution-to-rotation trail radius ratio trail, the following expression can be obtained:  $\omega_2 = (1 + \kappa)\omega_1$ .

The final position of a given point on the substrate can be derived as  $p' = R_1 D R_2 p$  [19].

### 3.3. Film thickness uniformity

By taking the integral of the film thickness distribution function along the path of the point  $p'$  on the substrate, the film thickness of the point within any time interval  $\tau$  can be obtained. To measure the uniformity of the film thickness, the uniformity degree of the coating, denoted as  $c$ , can be defined as:

$$c = (T_{\max} - T_{\min}) / T_{\text{mean}}, \quad (10)$$

where  $T_{\max}$  and  $T_{\min}$  are the maximum and minimum values of the relative film thickness on the substrate, respectively. Smaller values of  $c$  indicate higher coating film uniformity.

## 4. RESULTS AND DISCUSSION

By performing numerical analysis on the uniformity  $c$  with MATLAB, the change in the film thickness uniformity degree  $c$  with the number of revolution cycles was plotted in Fig. 6. When the number of revolution cycles exceeded 50, the uniformity showed a slight variation. Therefore, the boundary conditions with 50 cycles were used in the subsequent calculations.

At the revolution-to-rotation radius ratio  $\kappa > 2$ , the uniformity showed slight variation. The boundary condition  $\kappa$  was set to a value between 2 and 5 to simplify the calculation process. Meanwhile, the change in the uniformity under different eccentric distances and different radius ratios was also examined, with the final calculation results shown in Fig. 7. Assuming that  $e$  is the eccentric distance,  $e$  can be calculated as  $e = r - \chi - l$ , where  $r$  is the vacuum chamber radius ( $r = 2750$  mm),  $l$  is the target length, and  $\chi$  is the target spacing.

As shown in Fig. 7, as the eccentric distance  $e$  increased steadily (corresponding to the steady decrease in  $\chi$ ), the uniformity degree  $c$  dropped, i.e., the uniformity could be enhanced.

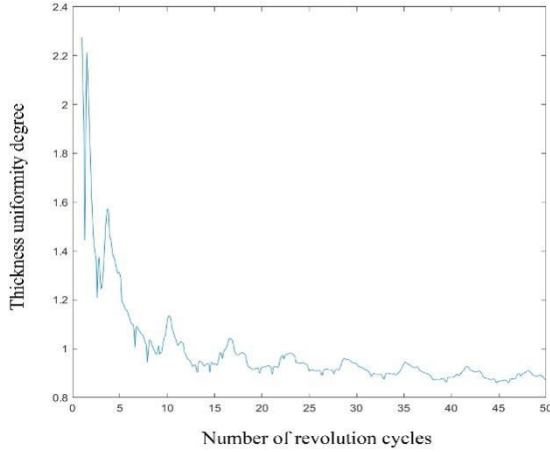


**Fig. 6.** Evolution of the film thickness uniformity with the number of revolution cycles

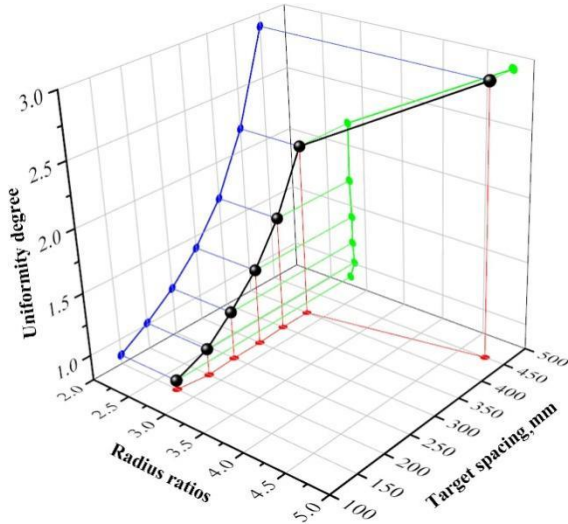


**Fig. 7.** Variations in the uniformity degree with the revolution-to-rotation radius ratio and the eccentric distance

The radius ratio should be maintained at approximately 2.8 at a fixed eccentric distance to achieve favorable uniformity. Accordingly, at  $e = 400$  mm ( $\chi = 150$  mm) and  $\kappa = 2.78$ , the uniformity degree  $c$  was 0.873, with a deviation of  $\pm 43\%$ , implying the most favorable uniformity. These findings are consistent with some previous research but offer a more detailed analysis of the parameters affecting uniformity [20–23].

Under that uniformity degree, the relative film thickness distribution of the planetary-motion substrate was calculated via normalization, and the motion path of the point on the substrate was plotted in Fig. 8.

It can be observed from Fig. 8 that the film thickness distribution on the substrate overall showed an umbrella pattern, with slight sinking at the center. The film thickness dropped gradually from the center to the edge. The relative film thickness values at the center and the edge were 55 and 10, respectively.

Fig. 9 shows the motion paths of different fixed points along the radial direction. Overall, the motion paths of

different fixed points showed consistent sparsity and were only densely distributed in the inner ring.

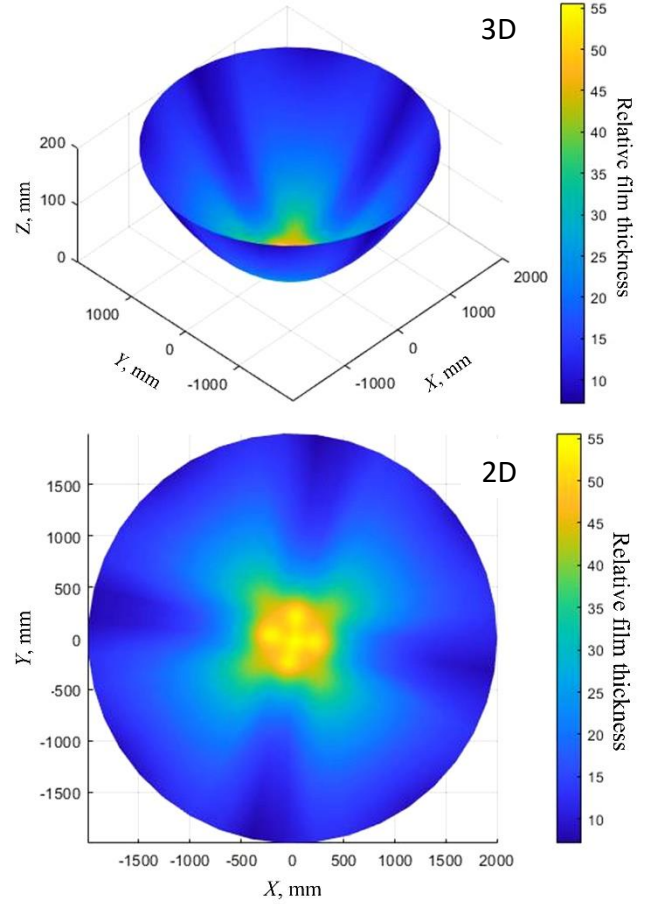


**Fig. 8.** Relative film thickness distribution patterns

As the radius of the radial fixed point increased, the coverage area of the motion path expanded steadily, and the relative path density dropped. When the radius of the fixed point was below 1000 mm, the motion paths mostly covered the region with a radius of 500 mm. Accordingly, in the region with a thicker film, the film thickness dropped along the radial direction, but the film thickness showed a smaller deviation and better uniformity.

## 5. CONCLUSIONS

This study focused on the uniformity of the film thickness on a large-scale curved workpiece using rectangular target magnetron sputtering. We established mathematical and physical models of the film thickness distribution and compared our findings with existing literature and expectations. The following conclusions can be drawn based on the results obtained in this study:

1. For rectangular magnetron-sputtering targets, the film thickness uniformity on the substrate along the target length direction was better than that along the target width direction. The uniformity along the target width direction primarily determined the film thickness uniformity.
2. In the sputtering system with eccentric composite revolution and rotation, the film thickness distribution can be changed by adjusting the revolution-to-rotation radius ratio and the eccentric distance.



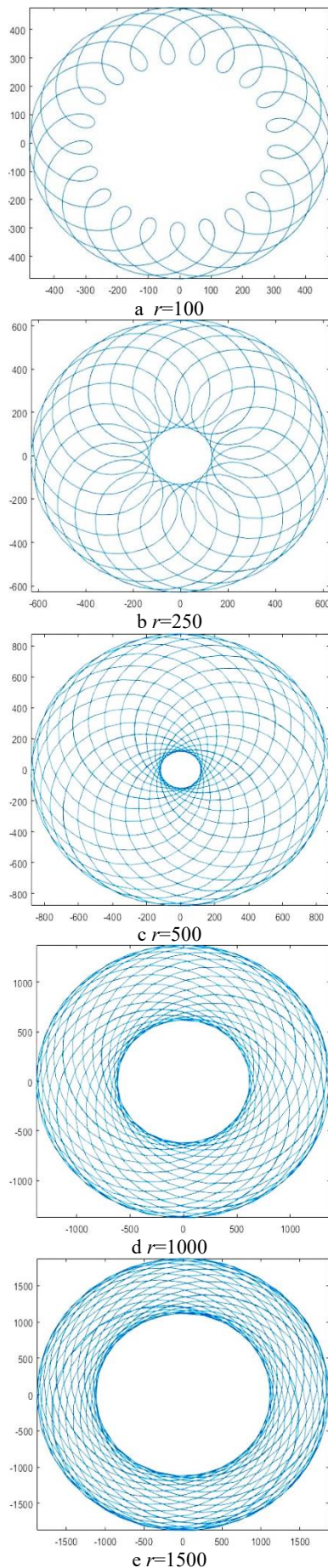


**Fig. 9.** Illustration of the motion paths of the fixed point on the substrate

At a radius ratio  $\kappa > 2$ , the uniformity degree varied within a small range. As the eccentric distance  $e$  increased steadily (corresponding to the decrease in target spacing), the uniformity degree  $c$  dropped, i.e., the uniformity degree was enhanced. When the eccentric distance was fixed, the radius ratio  $\kappa$  should be maintained at approximately 2.8 to achieve a favorable uniformity degree.

- At  $e = 400$  mm and  $\kappa = 2.78$ , the uniformity degree  $c$  was 0.873, indicating the most favorable uniformity. This result provides a practical guideline for those aiming to achieve optimal film thickness uniformity in similar setups.
- The motion paths of different fixed points along the radial direction affected the distribution of film thickness. For the fixed points, at a radius of below 1000 mm, the motion paths were mainly distributed in the annular region with a radius of 100 ~ 1500 mm. When the radius of the fixed points exceeded 1000 mm, no motion path was found in the region at a radius of over 500 mm; meanwhile, the circular region with no distribution of motion paths expanded gradually and the annular region including the motion paths developed gradually along the radial direction. Therefore, the motion paths were densely distributed in the region with a radius of 500 mm, in which more sputtered particles were received and the film was thickest. At a radius of over 500 mm, the motion paths were sparsely distributed, and the film thickness overall decreased; but the deviation of film thickness was small, suggesting favorable uniformity. The conclusion validated the thickness distribution corresponding to the best uniformity.

In conclusion, while our results corroborate some of the findings from previous research, they also provide new insights into the factors affecting film thickness uniformity in magnetron sputtering systems. Future studies might delve deeper into the reasons behind these observations and their implications for industrial applications.

### Acknowledgments

Lanzhou Talent Entrepreneurship and Innovation Project.

### REFERENCES

- Rother, B., Ebersbach, G., Gabriel, H.M.** Substrate-Rotation Systems and Productivity of Industrial PVD Processes *Surface & Coatings Technology* 116–119 1999: pp. 694–698.  
[https://doi.org/10.1016/s0257-8972\(99\)00120-6](https://doi.org/10.1016/s0257-8972(99)00120-6)
- Sassolas, B., Flaminio, R., Franc, J., Michel, C., Montorio, J.L., Morgado, N., Pinard, L.** Masking Technique for Coating Thickness Control on Large and Strongly Curved Aspherical Optics *Applied Optics* 48 (19) 2009: pp. 3760–3765.  
<https://doi.org/10.1364/ao.48.003760>
- Sassolas, B., Benoît, Q., Flaminio, R., Forest, D., Franc, J., Galimberti, M., Lacoudre, A., Michel, C., Montorio, J.L., Morgado, N., Pinard, L.** Thickness Uniformity Improvement for the Twin Mirrors Used in Advanced Gravitational Wave Detectors *Proceedings of SPIE*

8168 2011: pp. 81681Q.

<https://doi.org/10.1117/12.896318>

4. **Oliver, J.B., Talbot, D.** Optimization of Deposition Uniformity for large-aperture National Ignition Facility Substrates in a Planetary Rotation System *Applied Optics* 45 (13) 2006: pp. 3097–3105.  
<https://doi.org/10.1364/ao.45.003097>
5. **Cheng, C.J., Ming, H.C.** Studying Layer Uniformity of Sputter Coatings by Intensity Distribution of Plasma Spectrum *Applied Surface Science* 169–170 2001: pp. 649–653.  
[https://doi.org/10.1016/s0169-4332\(00\)00805-9](https://doi.org/10.1016/s0169-4332(00)00805-9)
6. **Bell, J.W.** Thickness Uniformity of Uranium Oxide Films Sputtered While Undergoing Planetary Motion. Ph. D. Thesis. Provo, Utah, USA: BrighamYoungUniversity, 2012: pp. 16–27.
7. **Zhang, Y.C., Song, Q.Z., Sun, Z.L.** Research on Thin Film Thickness Uniformity for Deposition of Rectangular Planar Sputtering Target *Physics Procedia* 32 2012: pp. 903–913.  
<https://doi.org/10.1016/j.phpro.2012.03.655>
8. **Silva, M.F.V., Nicholls, J.R.** A Model for Calculating the Thickness Profile of TiB<sub>2</sub> and Al Multilayer Coatings Produced by Planar Magnetron Sputtering *Surface and Coatings Technology* 142–144 2001: pp. 934–938.  
[https://doi.org/10.1016/s0257-8972\(01\)01257-9](https://doi.org/10.1016/s0257-8972(01)01257-9)
9. **Panjan, M., Cekada, M., Panjan, P.** Sputtering Simulation of Multilayer Coatings in Industrial PVD System with Three-Fold Rotation *Vacuum* 42 (82) 2008: pp. 158–161.  
<https://doi.org/10.1016/j.vacuum.2007.07.053>
10. **Shishkov, M., Popov, D.** Thickness Uniformity Of Thin Films Deposited on a Flat Substrate by Sputtering of A Target with Rotational Symmetry *Vacuum* 42 1991: pp. 1005.  
[https://doi.org/10.1016/0042-207x\(91\)90008-7](https://doi.org/10.1016/0042-207x(91)90008-7)
11. **Fu, C.L.F., Yang, C.R.** The Thickness Uniformity of Films Deposited by Magnetron Sputtering with Rotation and Revolution *Surface & Coatings Technology* 36 2006: pp. 87–89.  
<https://doi.org/10.1016/j.surfcoat.2004.12.023>
12. **Gross, M., Dligatch, S., Chtanov, A.** Optimization of Coating Uniformity in An Ion Beam Sputtering System Using A Modified Planetary Rotation Method *Applied Optics* 50 (9) 2011: pp. C316–C320.  
<https://doi.org/10.1364/ao.50.00c316>
13. **Jiang, C.Z., Zhu, J.Q., Han, J.C., Lei, P., Yin, X. B.** Uniform Film in Large Areas Deposited by Magnetron Sputtering with A Small Target *Surface & Coatings Technology* 229 (9) 2013: pp. 222–225.  
<https://doi.org/10.1016/j.surfcoat.2012.03.075>
14. **Tien, C.L., Cheng, K.S.** Improving Thickness Uniformity of Amorphous Oxide Films Deposited on Large Substrates by Optical Flux Mapping *Applied Sciences* 12 2022: pp. 11878.  
<https://doi.org/10.3390/app122311878>
15. **Shon, C.H., Lee, J.K.** Modeling of Magnetron Sputtering Plasmas *Applied Surface Science* 192 2002: pp. 258–269.  
[https://doi.org/10.1016/s0169-4332\(02\)00030-2](https://doi.org/10.1016/s0169-4332(02)00030-2)
16. **Mahieu, S., Buyle, G., Depla, D.** Monte Carlo Simulation of the Transport of Atom in DC Magnetron Sputtering *Nuclear Instruments and Methods in Physics Research B* 243 2006: pp. 313.  
<https://doi.org/10.1016/j.nimb.2005.09.018>
17. **Qi, H.F., Li, Q.Z.** A Cross-Corner Effect in a Rectangular Sputtering Magnetron *Journal of Physics D: Applied Physics* 36 2003: pp. 244–251.  
<https://doi.org/10.1088/0022-3727/36/3/305>
18. **Broadway, D.M., Kriese, M.D., Platonov, Y.Y.** Controlling Thin Film Thickness Distributions in Two Dimensions *SPIE* 4145 2001: pp. 80–87.  
<https://doi.org/10.1117/12.411623>
19. **Huang, Y., Gao, S.T., Liu, M.** Research of Film Uniformity on Vacuum Coating by Magnetron Sputtering with Multi-Sites *Advanced Engineering Forum* 2–3 2011: pp. 1082–1087.  
<https://doi.org/10.4028/www.scientific.net/AEF.2-3.1082>
20. **Fancey, K. S.** A Coating Thickness Uniformity Model for Physical Vapor Deposition Systems: Overview *Surface and Coatings Technology* 71 1995: pp. 16–29.
21. **Swann, S., Collett, S.A., Scarlett, I.R.** Film Thickness Distribution Control with Off-Axis Circular Magnetron Sources Onto Rotating Substrate Holders: Comparison of Computer Simulation with Practical Results *Journal of Vacuum Science and Technology A* 8 1990: pp. 1299–1303.  
<https://doi.org/10.1116/1.576871>
22. **Wang, B., Fu, X., Song, S., Chu, H., Gibson, D., Li, C., Shi, Y., Wu, Z.** Simulation and Optimization of Film Thickness Uniformity in Physical Vapor Deposition *Coatings* 8 2018: pp. 325.  
<https://doi.org/10.3390/coatings8090325>
23. **Savale, P.A.** Physical Vapor Deposition (PVD) Methods for Synthesis of Thin Films: A Comparative Study *Archives of Applied Science Research* 8 (5) 2016: pp. 1–8.



© Jiang et al. 2024 Open Access This article is distributed under the terms of the Creative Commons Attribution 4.0 International License (<http://creativecommons.org/licenses/by/4.0/>), which permits unrestricted use, distribution, and reproduction in any medium, provided you give appropriate credit to the original author(s) and the source, provide a link to the Creative Commons license, and indicate if changes were made.